



Research Journal of **Microbiology**

ISSN 1816-4935



Academic
Journals Inc.

www.academicjournals.com

Synthesis of Polyelectrolyte Nanoparticles from Anticancer Exopolysaccharide Isolated from Probiotic *Lactobacillus acidophilus*

^{1,2}Venkataraman Deepak, ¹Sureshbabu Ram Kumar Pandian, ²Shiva D. Sivasubramaniam, ¹Hariharan Nellaiah and ¹Krishnan Sundar

¹Department of Biotechnology, Kalasalingam University, Krishnankoil, 626126, Tamilnadu, India

²School of Science and Technology, Nottingham Trent University, Nottingham NG11 8NS, UK

Corresponding Author: Krishnan Sundar, Department of Biotechnology, Kalasalingam University, Krishnankoil, Tamilnadu, 626126, India Tel: + 91-4563-289042 Fax: +91-4563-289322

ABSTRACT

The composition of Exopolysaccharides (EPS) synthesized by *L. acidophilus* was analyzed by HPLC and found to contain glucose and galactose in the ratio of 1.43:1. The EPS was also found to contain sulfur, form stable emulsions in paraffin oil and flocculate activated charcoal. When the MCF-7 cells were treated with EPS, dose dependent reduction in survival was observed. The treated cells were found to have round and shrunken morphology. When the cells were stained with DAPI, nucleus with reduced size could be observed. EPS was then used to synthesize polyelectrolyte nanoparticles with chitosan. The nanoparticles were checked with FTIR spectroscopy, Dynamic Light Spectral (DLS) analysis and Transmission Electron Microscopic (TEM) analysis. The DLS measurement showed that the size of the nanoparticles to be 94.6 ± 7.8 nm. When the entrapment ability of the nanoparticle was evaluated with Nile red, a maximum of $74.7 \pm 1.26\%$ entrapment could be observed.

Key words: Exopolysaccharide, characterization, anticancer, polyelectrolyte nanoparticles

INTRODUCTION

Polyelectrolyte nanoparticles are synthesized when two opposite charged natural polymers interact with each other reversibly (Hamman, 2010). Recently considerable attention has been given to biodegradable nanoparticles since, they have higher surface area, protect the drugs from degradation and can be useful in delivering the drugs through various routes of administration (Lemarchand *et al.*, 2003). Polysaccharides have been recently focused, as they are biodegradable, hydrophilic and biocompatible and can be used for the production of polyelectrolyte nanoparticles for drug loading and delivery (Sarmiento *et al.*, 2006). Exopolysaccharide is a kind of natural polymer made up of sugar, produced by various organisms that is either loosely bound to the external cell surface or secreted out into the surrounding environment (Han *et al.*, 2014).

Exopolysaccharides (EPS) have number of applications in food, pharmaceutical and various other industries. The EPS is used for flocculation (Han *et al.*, 2014), emulsification (Han *et al.*, 2015), for enhancing the texture of food (Badel *et al.*, 2011) and as a gelling agent (Ruas-Madiedo *et al.*, 2002). EPS have been reported to have two functions that include protection of cells under adverse environments and colonization of the cells in various ecosystems (Wang *et al.*, 2014). Various probiotic Lactic Acid Bacteria (LAB) also synthesize EPS. Probiotic

bacteria are those which administered in adequate amounts results in benefitting the health of the individual. Several modes have been proposed for the beneficial effects of the probiotic bacteria which include competitive exclusion of the disease causing bacteria, strengthening the epithelial barrier of the intestine, immunomodulation and removal of the carcinogens (Tripathi *et al.*, 2012). Although the amount of EPS produced by LAB is comparably less, most of the bacteria fall into the category of Generally Regarded As Safe (GRAS), as they are food grade organisms (Badel *et al.*, 2011). Researches for various natural anticancer agents have been performed and EPS which has been reported to possess anti tumor activity, is one among them. Though, there are many synthetic anti-tumor agents available, they are not only expensive but their compatibility in the long run is in a state of uncertainty (Choi *et al.*, 2006). ESP were previously reported to reduce the survival of various cancer cell lines including liver, gastric, breast and colon cancer (Choi *et al.*, 2006; Wang *et al.*, 2014).

Chitosan is a deacetylated form of chitin, the second most abundant natural polymer. Chitosan is composed of D-glucosamine and N-acetylglucosamine. Chitosan is found to be nontoxic for human and has widely been used in the food industry. It has been converted to thin edible films for protection against microorganisms (Coma *et al.*, 2002). Chitosan itself was previously converted to nanoparticles and tested for delivering various drugs (Tiyaboonchai, 2003). In the present study, the composition of the EPS produced by *L. acidophilus* was determined using HPLC, the effect of EPS on MCF-7 cells were analyzed, polyelectrolyte nanoparticles were synthesized using EPS and chitosan; they were characterized and their entrapment efficiency was determined.

MATERIALS AND METHODS

Organism and culture conditions: *Lactobacillus acidophilus* (10307) was acquired from Microbial Type Culture Collection (MTCC), IMTECH, Chandigarh, India. The organism was maintained in slants at 4°C, renewed every two weeks in MRS agar (Hi-Media, India) and used for experiments. Exopolysaccharides were essentially synthesized using the optimized medium (Sucrose 3%, Yeast extract 1%, mixture of salts (MgSO₄ and CaCl₂) 0.2%, NaCl 1% incubated at 37°C for 24 h), extracted and purified as reported earlier (Deepak *et al.*, 2015).

Determination of degree of sulfation: The degree of sulfation of EPS from *L. acidophilus* was determined as reported earlier (Dodgson and Price, 1962). Initially, 20 mg of EPS sample was dissolved in water along with 1N HCl. The mixture was heated at 100°C for 4 h. To 0.2 mL of this heated mixture, 3.8 mL of 4% TCA (trichloroacetic acid) was added, followed by the addition of 1 mL of barium chloride-gelatin solution (1:1) and incubated at room temperature for 20 min. Another mixture was prepared where, instead of barium chloride-gelatin solution, a 0.5% gelatin solution was used. The transmittance was measured at 360 nm. A stock solution of potassium sulfate was used as the standard.

Characterization of EPS by HPLC: The EPS was characterized by the method given by Yang *et al.* (2005). 2.0 mg of EPS was dissolved in 2 mL of 4 M trifluoroacetic acid in a screw capped autoclavable tube and heated to 110°C in an oil bath for 8 h. The reaction mixture after cooling was centrifuged at 1000 rpm and later neutralized by the addition of 0.3 M NaOH. This mixture was then used for derivatization with 1-phenyl-3-methyl-5-pyrazolone (PMP). The hydrolyzed sample was mixed with 0.5 M PMP dissolved in methanol (1:1 ratio). The mixture was then heated to 70°C for 30 min and neutralized with 0.3 M HCl. Later the PMP derivatized mixture was mixed

vigorously with excess of chloroform. Excess reagents will be removed with chloroform and the aqueous layer was further extracted thrice. The resulting aqueous layer was filtered through 0.22 µm filter (Millipore Inc., USA) diluted with water and analyzed by HPLC instrument (Shimadzu, Japan) at 245 nm, in a C₁₈ column 250×4.16 mm, stainless steel column packed with Octadecylsilane (C₁₈) bonded to porous silica. The flowrate was maintained at 1.5 mL min⁻¹ and the injected volume is 20 µL.

Thermogravimetric analysis (TGA) of EPS: For TGA, 15 mg vacuum dried EPS was analyzed using SDT Q600 V8.3 Build 101 TGA apparatus (TA Instruments, USA) with temperature ranging 0-800°C and the rate of change in temperature is 10°C min⁻¹. The resulting curve obtained from TGA signal was converted to mass change at y-axis with the temperature of material plotted on the x-axis.

Analysis of emulsification activity of EPS: To analyze the emulsifying activity, EPS was dissolved in deionized water (0.5 mg mL⁻¹) and mixed with paraffin oil in the ratio of 2:3 followed by mixing in a vortex for 5 min. The mixture was then left undisturbed for 24 h, after which the emulsion index (E₂₄) was determined using the formula:

$$E_{24} = \frac{h_e}{h} \times 100$$

where, h_e is the height of the emulsion layer after 24 h and h is the total height of the mixture.

Analysis of flocculation activity of EPS: The flocculating activity of EPS was determined using activated charcoal. A mixture was prepared by mixing 50 mg of charcoal in 10 mL of deionized water followed by the addition of 0.1 mL of CaCl₂.2H₂O solution (6.5 mM). The experiment was performed with various concentrations of EPS (0.125-1 mg mL⁻¹). The mixture was then mixed in a vortex for 30 sec and left undisturbed for 10 min. The upper phase (1 mL) was removed and its absorbance (A_s) read at 550 nm. Xanthan gum was used as the positive control and the negative control was the reaction mixture without either EPS or xanthan gum (A_c). The percentage of flocculating activity was calculated based on the formula:

$$\text{Flocculating activity (\%)} = \frac{AC - AS}{AC} \times 100$$

Cell line and treatment conditions: MCF-7 cell line was used for the experiment. It was maintained in EMEM supplemented with 10% serum. To determine the effect of EPS on MCF-7 cells under normoxic conditions, cells were seeded into 96 well plate and treated with various concentrations of EPS for 48 h. The changes in the morphology of the cells were determined by phase contrast microscopy and fluorescent microscopy. For fluorescent microscopy, cells were pelleted by centrifugation and the supernatant was removed. The pelleted cells were stained with DAPI and visualized in a fluorescent microscope (excitation 355 nm and emission 455 nm) (Olympus, USA).

Preparation of EPS-Chitosan (EPSCH) nanoparticles: The EPSCH nanoparticles were spontaneously synthesized by the method that has been reported earlier (Raveendran *et al.*, 2013).

The method involves mixing of EPS, dissolved in distilled water and Chitosan, dissolved in 1% acetic acid in the ratio of 1:1.25 under constant magnetic stirring. Then the synthesized nanoparticles were subjected to characterization by various methods.

Characterization of nanoparticles

FT-IR: In order to characterize the EPS, Chitosan and EPSCH nanoparticles, they were initially dried in a vacuum dessicator. The dried powder was then subjected to analysis in a FT-IR analyzer (IR Tracer, 100, Shimadzu) in the range 400-4000 cm^{-1} . The obtained peaks were compared with the control and the resulting compounds were analyzed.

DLS analysis: The diameter and the size distribution of the EPSCH nanoparticles were initially measured by the Dynamic Light Scattering (DLS) method in HORIBA SZ-100 particle size analyzer. The detector scattering angle was fixed at 90° and the temperature at 25°C.

Transmission electron microscopic imaging: The morphology of the nanoparticle was determined by transmission electron microscopy. The nanoparticles were negatively stained with 2% phosphotungstic acid and placed on carbon coated copper grid. The particles were then examined in JOEL JEM 1400 transmission electron microscope operating under an accelerating voltage of 80 kV. The micrographs of the nanoparticles were obtained using Olympus Keenview CCD camera attached to the microscope.

Determination of entrapment efficiency: Nile Red (NR) was used as a marker for the determination of the entrapment capacity of the nanoparticles. Initially NR was dissolved in ethanol and added to chitosan solution to get final concentrations of 0.0025, 0.005, 0.0075 and 0.010 mg mL^{-1} . To analyze the entrapment efficiency, the nanoparticles synthesized were centrifuged at 14000 rpm for 30 min; the collected pellet was resuspended in ethanol and sonicated for 20 sec. The solution was further centrifuged at 14000 rpm for 30 min and the supernatant was analyzed in a spectrophotometer at 575 nm (Shimadzu, Japan). Ethanol was used as the blank.

RESULTS AND DISCUSSION

A media for the optimization of EPS production from *L. acidophilus* has been reported previously (Deepak *et al.*, 2015). Here the EPS was extracted, purified and converted to polyelectrolyte nanoparticles with chitosan.

Estimation of sulfate content: EPS from *L. acidophilus* was found to contain 8.8% of sulfate. The presence of sulfur was also checked using FT-IR, where vibrations near 1270 cm^{-1} and 1225 cm^{-1} , already reported for sulfur ester groups, were observed. Polysaccharides with sulfur ester have been found to possess many bioactive properties that include antioxidative and anticancer properties (De Souza *et al.*, 2007; Raveendran *et al.*, 2013).

HPLC analysis of EPS: The hydrolyzed monosaccharides of EPS has been analyzed with HPLC and compared with the standard sugars. Two peaks at the R_f value of 11.38 and 11.95 sec were prominent in HPLC profile which corroborated with that of glucose and galactose. An initial peak at 3.26 sec was also obtained which corresponds to the PMP (Fig. 1). When EPS from various organisms were characterized, it was found to contain glucose and galactose which include

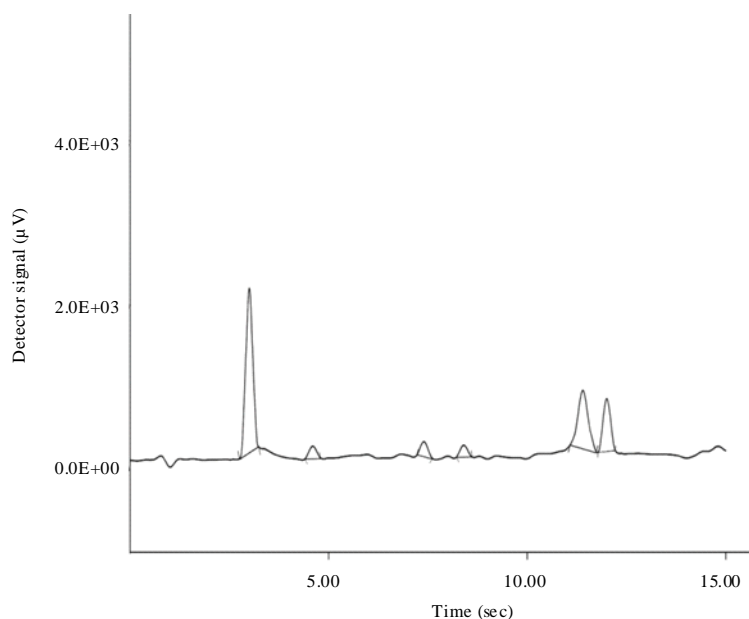


Fig. 1: HPLC chromatogram for EPS from *L. acidophilus*. The peaks at 11.38 and 11.95 sec correspond to glucose and galactose, respectively

L. delbrueckii subsp. *Bulgarius* (Grobben *et al.*, 1996), *L. rhamnosus* (Gamar *et al.*, 1997) and *L. fermentum* F6 (Zhang *et al.*, 2011). In all the aforesaid studies, EPS was reported to be made up of glucose and galactose alone.

The ratio of glucose and galactose in the EPS was found to be 1.43:1. The ratio of the sugars were found vary in different organisms: 1:2.4 in *L. delbrueckii* subsp. *Bulgarius* (Grobben *et al.*, 1996), 1:1 in *L. rhamnosus* (Gamar *et al.*, 1997) and 2.5:1 in *L. fermentum* F6 (Zhang *et al.*, 2011). This corroborate with the present observation.

TGA analysis: TGA curve basically gives an idea of the thermal stability of the material. When the purified EPS was subjected to TGA, the material was found to be stable up to 217°C and then started to degrade (Fig. 2). Up to 80% EPS was stable up to 217°C. The stability of the EPS was greatly reduced at temperatures more than 400°C and at nearly 500°C, 30% of the initial mass of the EPS remained. The degradation was found to contain two phases where the initial phase was gradual resulting in 43% degradation and the second acute phase resulting in the degradation of remaining mass of 26%. Similar temperatures of stability were also reported for various EPS. Exopolysaccharides (EPS) from *Pleurotus pulmonarius* was also found to have stability up to 217°C (Shen *et al.*, 2013). EPS from *Pseudozyma* sp. was found to have stability up to 220°C (Sajna *et al.*, 2013).

Emulsifying activity of EPS on paraffin oil: In order to study the effect of EPS on the emulsification stability, emulsions for the various concentrations of EPS were prepared with paraffin oil. There was an increase in the E_{24} values up to 0.5 mg mL⁻¹ of EPS and up to 0.625 mg mL⁻¹ of xanthan gum, after which the values were stable, with no significant differences observed (Fig. 3). An earlier study by Prasanna *et al.* (2012) has also shown the same trend in the emulsification index of EPS isolated from *Bifidobacterium longum*, a probiotic bacterium, with

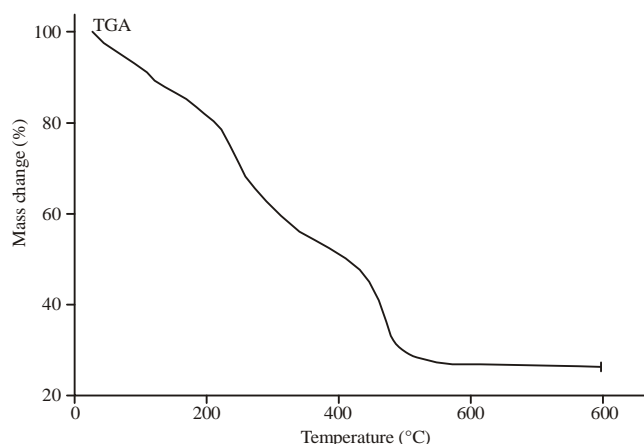


Fig. 2: TGA spectrum of EPS obtained from *L. acidophilus* with rate of heating at $10^{\circ}\text{C min}^{-1}$

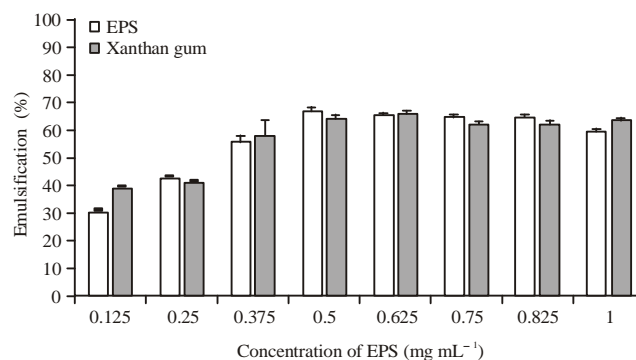


Fig. 3: Emulsification activities of EPS. EPS increased emulsification of paraffin oil upto 0.5 mg mL^{-1} after which there was no significant difference

sunflower oil. According to them, the emulsification index increased up to 1 mg mL^{-1} of EPS, after which it was stable. Figure 4 shows the micrographs of emulsion obtained from EPS and paraffin oil at 0 and 24 h. Initially, the particle size of the emulsion was large and this decreased after 24 h. The droplet size in the emulsion is reported to be important for the stability of the emulsion and also for other properties like flocculation and creaming rate. The emulsion prepared from EPS in the present study was found to have a narrower droplet size distribution compared with that of xanthan gum.

Flocculating activity of EPS: The ability of EPS to flocculate activated charcoal was examined. As shown in Fig. 5, when the concentration of EPS was increased ($0.125\text{-}1 \text{ mg mL}^{-1}$), the ability to flocculate decreased. Currently, biologically produced flocculants are more focused upon in view of their biodegradability and non-toxicity (Das *et al.*, 2014). The maximum flocculating activity of EPS was obtained at a concentration of 0.125 mg mL^{-1} ($79.32 \pm 0.87\%$) and when the concentration was increased further, the percentage of flocculation decreased. The same pattern of flocculating activity was obtained for EPS isolated from bacteria, *Zoogloea* sp. (Lim *et al.*, 2007). Flocculants are highly useful in food processing, wastewater treatment, fermentation and downstream processing (Han *et al.*, 2014).

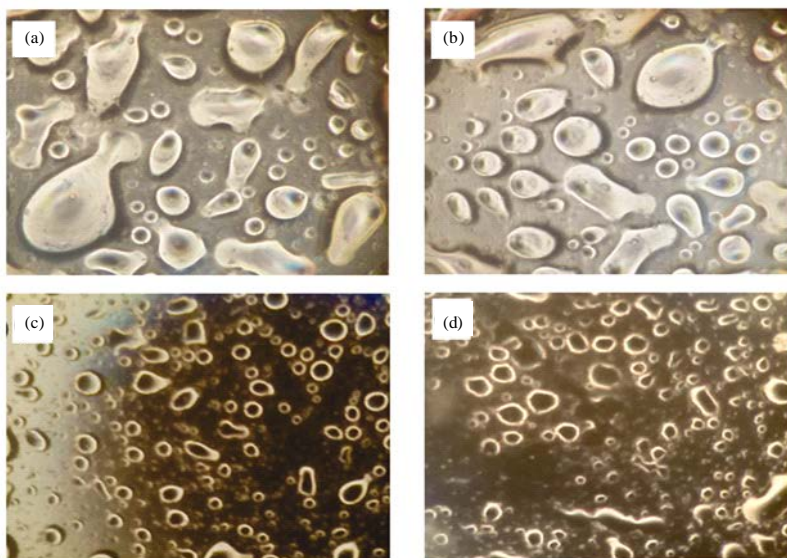


Fig. 4(a-d): Phase contrast microscopic images of emulsions. Emulsions formed were subjected to phase contrast microscopy (10×), where emulsions formed by (a, c) EPS at 0 h and (b, d) Xanthan gum at 24 h, respectively

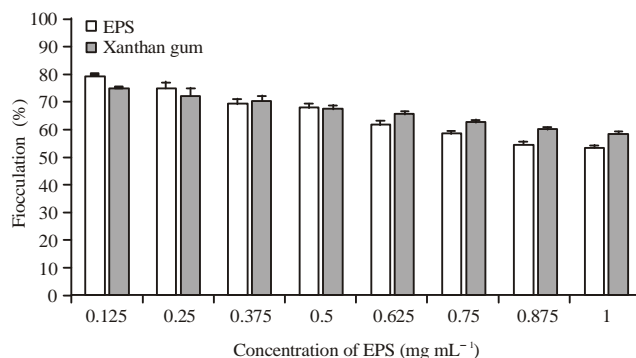


Fig. 5: Flocculating activity of EPS. EPS on increase in the concentration reduced the flocculation of activated charcoal

EPS induces cell death in MCF-7 cell line: MCF-7 cells were treated with various concentrations of EPS. As the concentration of EPS was increased, the survival of the MCF-7 cells were reduced (Fig. 6). Later, when the cells were visualized under a phase contrast microscope, the EPS treated cells showed a shrunken morphology when compared to untreated control cells (Fig. 7). The MCF-7 cells treated with EPS and stained with DAPI are shown in Fig. 7. The control cells showed clear intact nucleus, as it can be seen from the bright blue fluorescence in Fig. 7 and the EPS treated cells showed the shrunk nucleus (Fig. 7). This is in corroboration with previous reports that have shown that EPS from various *Lactobacillus* sp. has antitumor activities (Choi *et al.*, 2006; Liu *et al.*, 2011; Wang *et al.*, 2014).

Polyelectrolyte nanoparticle formulation and its characterization: Polyelectrolyte nanoparticles were synthesized by the mixing of EPS from *L. acidophilus* and Chitosan. Previously,

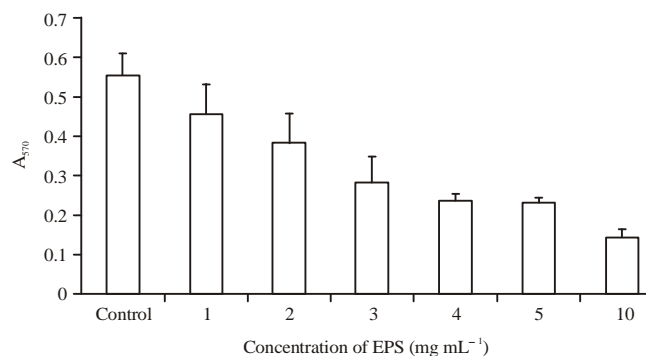


Fig. 6: EPS reduced the cell survival in MCF-7 cells. MCF-7 cells treated with various concentrations of EPS, where, increase in concentration of EPS was found to reduce the survival of the MCF-7 cell line

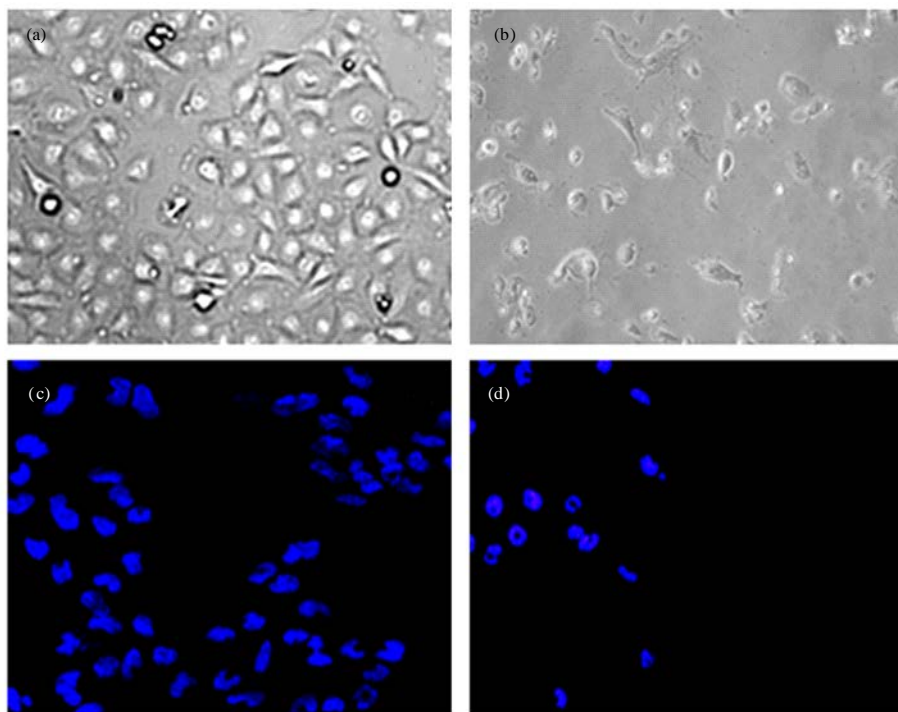


Fig. 7(a-d): (a, b) Phase contrast microscopic images which correspond to the control and EPS treated MCF-7 cells; where shrunken and rounded cells of MCF-7 during EPS treatment could be visualized when compared with untreated control and (c, d) Fluorescent microscopic images correspond to the control and EPS treated MCF-7 cells, where nucleus was found be dislodged and fragmented when compared with the untreated control where healthy could be visualized

Chitosan alone has been converted to nanoparticle and applied for various applications. It was found to be non-toxic, biodegradable and biocompatible (Illum, 1998). Chitosan has been

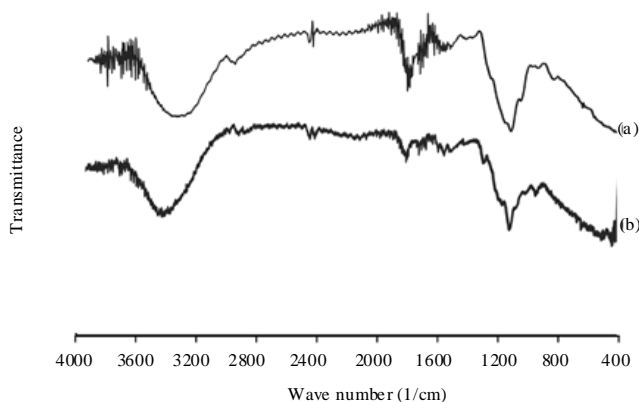


Fig. 8: FTIR spectrogram for (a) Chitosan and (b) EPSCH nanoparticles

converted to nanoparticles along with various other polymers such as dextran sulphate for insulin immobilization (Sarmiento *et al.*, 2006) and muran for cancer drug delivery and bioimaging (Raveendran *et al.*, 2013). Here, EPS and chitosan were coupled to form EPSCH nanoparticles and it has been characterized by FT-IR, DLS and TEM analysis.

FT-IR studies: The characteristic peak for purified EPS has been previously reported (Deepak *et al.*, 2015). The FTIR peaks for chitosan and EPSCH nanoparticles have been shown in Fig. 8. For chitosan a broad peak was obtained in the region of 3300 cm^{-1} is due to O-H stretching and a peak obtained in the region between 1000 and 1200 cm^{-1} correspond to C-O-C stretch and glycosidic linkage. Two peaks in the region of 1666 and 1712 cm^{-1} correspond to amide linkage and C = O stretching and a peak in the 2980 cm^{-1} is due to C-H stretching (Fig. 8). In EPSCH nanoparticles, the broad peak shifted 3400 cm^{-1} and the peak 1666 cm^{-1} might have shifted to 1612 cm^{-1} and peak 1712 cm^{-1} might have shifted to 1691 cm^{-1} (Fig. 8). Apart from these, there is a peak at 1435 cm^{-1} , because of NH stretching in chitosan is also present in EPSCH nanoparticle at 1431 cm^{-1} and a peak at 902 cm^{-1} may occur due to the β sugar configuration in EPS is also present at 912 cm^{-1} in EPSCH nanoparticle which may well serve to monitor the formation of nanoparticles (Bremer and Geesay, 1991; Sarmiento *et al.*, 2006; Wang *et al.*, 2010; Raveendran *et al.*, 2013).

Size determination: The average size of the nanoparticle was determined in the particle size analyzer and the average size of the nanoparticle was found to be $94.6 \pm 7.8\text{ nm}$ (Fig. 9 (inset)). Size distribution of the nanoparticle was found to be very less in EPSCH nanoparticle when analyzed by DLS analysis.

Visualization of nanoparticles in TEM: Electron microscopy is one of the vital tools in visualizing nanoparticles. The size of the EPSCH nanoparticle visualized by TEM is approximately 80 nm (Fig. 9), ranging from 40 - 120 nm which also corroborates with the results of DLS analysis. Most of the nanoparticles were spherical in shape and also other shapes could be found. Previously polyelectrolyte nanoparticles of different sizes have been reported for various applications. The average size of muran-chitosan nanoparticle is in the range of 30 - 200 nm (Raveendran *et al.*, 2013) and 400 nm for dextran sulphate-chitosan nanoparticle (Chaiyasan *et al.*, 2013).

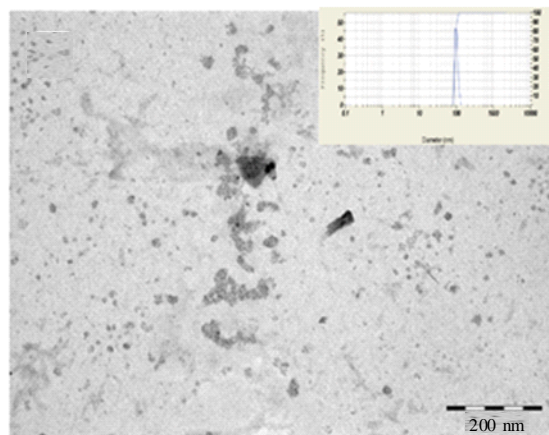


Fig. 9: TEM image of the negatively stained EPSCH nanoparticle, (inset) DLS spectrum of the EPSCH nanoparticle synthesized which shows the average size of the nanoparticles to be 94.6 ± 7.8 nm

Table 1: Entrapment efficiency of EPSCH nanoparticle at various concentrations of nile red

Concentration of nile red (mg mL^{-1})	Entrapment efficiency (%)
0.0025	58.62 ± 2.52
0.005	74.70 ± 1.26
0.0075	62.81 ± 2.79
0.001	58.96 ± 4.03

Entrapment efficiency of EPSCH nanoparticles: The entrapment efficiency of the EPSCH nanoparticle is given in the Table 1. A maximum of 74.70% of nile red was found to be entrapped in the EPSCH nanoparticles. Previously nanoparticles consisted of dextran sulphate-chitosan was tested for nile red and Rhodamine B entrapment and maximum efficiency of 83 and 82% was obtained, respectively. Polyelectrolyte nanoparticles have been reported to be safe as the components were associated based on the reversible electrostatic interactions along with hydrophobic and hydrogen bondings; unlike the polymers linked by chemicals which at times may induce toxicity owing to unreacted chemical cross linkers that require purification and verification steps. Added advantage of using EPS from probiotic bacteria and chitosan, which is nontoxic and the nanoparticles can be used to deliver the drugs orally which is the most preferred way (Luo and Wang, 2014). Apart from these various, other moieties like insulin and 5-fluorouracil has been immobilized on polyelectrolyte nanoparticles. The immobilized insulin and 5-FU have been released in a sustained manner warranting the application of the nanoparticles in medicinal field (Sarmiento *et al.*, 2007; Raveendran *et al.*, 2013).

CONCLUSION

EPS was found to contain glucose and galactose in its composition. The MCF-7 cells were found to have shrunk morphology when treated with EPS. ESP was converted to nanoparticles with chitosan and was characterized. Further studies are needed in order to determine the efficiency of the EPSCH nanoparticle for cancer treatment/drug delivery.

ACKNOWLEDGMENTS

The author DV thanks Council of Scientific and Industrial Research (CSIR), India for the senior research fellowship (Ref: 9/10/2(0001)2k10-EMRI). The authors also thank Dr. Pushpa Viswanathan, Cancer Institute (WIA), Chennai for help in TEM analysis.

REFERENCES

- Badel, S., T. Bernardi and P. Michaud, 2011. New perspectives for *Lactobacilli* exopolysaccharides. Biotechnol. Adv., 29: 54-66.
- Bremer, P.J. and G.G. Geesey, 1991. An evaluation of biofilm development utilizing non-destructive attenuated total reflectance Fourier transform infrared spectroscopy. Biofouling, 3: 89-100.
- Chaiyasan, W., S.P. Srinivas and W. Tiyafoonchai, 2013. Mucoadhesive chitosan-dextran sulfate nanoparticles for sustained drug delivery to the ocular surface. J. Ocular Pharmacol. Therap., 29: 200-207.
- Choi, S.S., Y. Kim, K.S. Han, S. You, S. Oh and S.H. Kim, 2006. Effects of *Lactobacillus* strains on cancer cell proliferation and oxidative stress *in vitro*. Lett. Applied Microbiol., 42: 452-458.
- Coma, V., A. Martial-Gros, S. Garreau, A. Copinet, F. Salin and A. Deschamps, 2002. Edible antimicrobial films based on chitosan matrix. J. Food Sci., 67: 1162-1169.
- Das, D., R. Baruah and A. Goyal, 2014. A food additive with prebiotic properties of an α -D-glucan from *Lactobacillus plantarum* DM5. Int. J. Biol. Macromol., 69: 20-26.
- De Souza, M.C.R., C.T. Marques, C.M.G. Dore, F.R.F. da Silva, H.A.O. Rocha and E.L. Leite, 2007. Antioxidant activities of sulfated polysaccharides from brown and red seaweeds. J. Applied Phycol., 19: 153-160.
- Deepak, V., S.R.K. Pandian, S.D. Sivasubramaniam, H. Nellaiah and K. Sundar, 2015. Optimization of anticancer exopolysaccharide production from probiotic *Lactobacillus acidophilus* by response surface methodology. Prep. Biochem. Biotechnol., 10.1080/10826068.2015.1031386
- Dodgson, K.S. and R.G. Price, 1962. A note on the determination of the ester sulphate content of sulphated polysaccharides. BioChem. J., 84: 106-108.
- Gamar, L., K. Blondeau and J.M. Simonet, 1997. Physiological approach to extracellular polysaccharide production by *Lactobacillus rhamnosus* strain C83. J. Applied Microbiol., 83: 281-287.
- Grobbs, G.J., M.R. Smith, J. Sikkema and J.A.M. De Bont, 1996. Influence of fructose and glucose on the production of exopolysaccharides and the activities of enzymes involved in the sugar metabolism and the synthesis of sugar nucleotides in *Lactobacillus delbrueckii* subsp. bulgaricus NCFB 2772. Applied Microb. Biotechnol., 46: 279-284.
- Hamman, J.H., 2010. Chitosan based polyelectrolyte complexes as potential carrier materials in drug delivery systems. Mar. Drugs, 8: 1305-1322.
- Han, P.P., Y. Sun, X.Y. Wu, Y.J. Yuan, Y.J. Dai and S.R. Jia, 2014. Emulsifying, flocculating and physicochemical properties of exopolysaccharide produced by cyanobacterium *Nostoc flagelliforme*. Applied Biochem. Biotechnol., 172: 36-49.
- Han, Y., E. Liu, L. Liu, B. Zhang and Y. Wang *et al.*, 2015. Rheological, emulsifying and thermostability properties of two exopolysaccharides produced by *Bacillus amyloliquefaciens* LPL061. Carbohydrate Polymers, 115: 230-237.
- Illum, L., 1998. Chitosan and its use as a pharmaceutical excipient. Pharm. Res., 15: 1326-1331.
- Lemarchand, C., P. Couvreur, M. Besnard, D. Costantini and R. Gref, 2003. Novel polyester-polysaccharide nanoparticles. Pharm. Res., 20: 1284-1292.

- Lim, D.J., J.D. Kim, M.Y. Kim, S.H. Yoo and J.Y. Kong, 2007. Physicochemical properties of the exopolysaccharides produced by marine bacterium *Zoogloea* sp. KCCM10036. J. Microbial. Biotechnol., 17: 979-984.
- Liu, C.F., K.C. Tseng, S.S. Chiang, B.H. Lee, W.H. Hsu and T.M. Pan, 2011. Immunomodulatory and antioxidant potential of *Lactobacillus* exopolysaccharides. J. Sci. Food Agric., 91: 2284-2291.
- Luo, Y. and Q. Wang, 2014. Recent development of chitosan-based polyelectrolyte complexes with natural polysaccharides for drug delivery. Int. J. Boil. Macromol., 64: 353-367.
- Prasanna, P.H.P., A. Bell, A.S. Grandison and D. Charalampopoulos, 2012. Emulsifying, rheological and physicochemical properties of exopolysaccharide produced by *Bifidobacterium longum* subsp. *infantis* CCUG 52486 and *Bifidobacterium infantis* NCIMB 702205. Carbohydrate Polymers, 90: 533-540.
- Raveendran, S., A.C. Poulouse, Y. Yoshida, T. Maekawa and D.S. Kumar, 2013. Bacterial exopolysaccharide based nanoparticles for sustained drug delivery, cancer chemotherapy and bioimaging. Carbohydrate Polymers, 91: 22-32.
- Ruas-Madiedo, P., J. Hugenholtz and P. Zoon, 2002. An overview of the functionality of exopolysaccharides produced by lactic acid bacteria. Int. Dairy J., 12: 163-171.
- Sajna, K.V., R.K. Sukumaran, L.D. Gottumukkala, H. Jayamurthy, K.S. Dhar and A. Pandey, 2013. Studies on structural and physical characteristics of a novel exopolysaccharide from *Pseudozyma* sp. NII 08165. Int. J. Boil. Macromol., 59: 84-89.
- Sarmiento, B., A. Ribeiro, F. Veiga and D. Ferreira, 2006. Development and characterization of new insulin containing polysaccharide nanoparticles. Coll. Surf. B: Biointerf., 53: 193-202.
- Sarmiento, B., A. Ribeiro, F. Veiga, P. Sampaio, R. Neufeld and D. Ferreira, 2007. Alginate/chitosan nanoparticles are effective for oral insulin delivery. Pharm. Res., 24: 2198-2206.
- Shen, J.W., C.W. Shi and C.P. Xu, 2013. Exopolysaccharides from *Pleurotus pulmonarius*: Fermentation optimization, characterization and antioxidant activity. Food Technol. Biotechnol., 51: 520-527.
- Tiyaboonchai, W., 2003. Chitosan nanoparticles: A promising system for drug delivery. Naresuan University J., 11: 51-66.
- Tripathi, P., A. Beaussart, G. Andre, T. Rolain and S. Lebeer *et al.*, 2012. Towards a nanoscale view of lactic acid bacteria. Micron, 43: 1323-1330.
- Wang, K., W. Li, X. Rui, X. Chen, M. Jiang, M. Dong, 2014. Characterization of a novel exopolysaccharide with antitumor activity from *Lactobacillus plantarum* 70810. Int. J. Biol. Macromol., 63: 133-139.
- Wang, Y., C. Li, P. Liu, Z. Ahmed, P. Xiao and X. Bai, 2010. Physical characterization of exopolysaccharide produced by *Lactobacillus plantarum* KF5 isolated from Tibet Kefir. Carbohydrate Polymers, 82: 895-903.
- Yang, X., Y. Zhao, Q. Wang, H. Wang and Q. Mei, 2005. Analysis of the monosaccharide components in *Angelica* polysaccharides by high performance liquid chromatography. Anal. Sci., 21: 1177-1180.
- Zhang, Y.U., S. Li, C. Zhang, Y. Luo, H. Zhang and Z. Yang, 2011. Growth and exopolysaccharide production by *Lactobacillus fermentum* F6 in skim milk. Afr. J. Biotechnol., 10: 2080-2091.